J. Sci. Math. Res. (2007) vol. 1, pp. 2-20 Published by Centaurus Press
(Received 2007-11-09; revised 2008-08-23)

A correlation between drag and an integral property of the wake

T. S. Morton

Department of Mechanical, Aerospace & Biomedical Engineering, University of Tennessee Space Institute
411 B.H. Goethert Parkway, Tullahoma, TN 37388, USA

An integral quantity is presented that relates the wake of a body in nominally two-dimensional flow to its drag, for Reynolds numbers ranging from 9,000 to 144,000. It is defined as the ratio of the kinetic energy to the vorticity in the fluid boundary and, for the special case of laminar flow, is proportional to the angular momentum in the wake bubble. The new quantity is useful for correlating drag data for cylinders, wedges, v-gutters, and normal flat plates with and without splitter plates. The correlation indicates that the drag force is proportional to the flow speed and the mass flow rate stored in the wake bubble. Order-of-magnitude arguments indicate that, absent any quantization of vortex size, this mass flow rate, and hence the drag force, can become unbounded as the size of the vortices contained in the wake becomes smaller.

1. Introduction

This paper proposes a new quantity useful in correlating aerodynamic drag of bluff bodies to flow properties of the near wake in the range: $9 \times 10^3 \leq Re \leq 1.44 \times 10^5$, (see Morton 1997). In the context of bluff-body flows, the quantity is the ratio of the kinetic energy (mean, periodic, and turbulent) to the vorticity in the wake of the body.

The long distances traveled by golf balls have been generally explained in terms of high momentum transport from the turbulent boundary layer (see Davies 1949). The drag reducing capability of riblets (see Walsh and Lindemann 1984, Coustols 1996) has likewise been explained in similar terms. However, Djenidi *et al.* (1994) found that appropriately sized riblets reduce frictional drag in *laminar* flows as well, at least on a per unit of wetted length basis.

Early discussions on the enhanced flying characteristics of spinning projectiles, enabled, for example, by the rifling of a gun barrel, focused primarily on gyroscopic stability (Milne-Thomson 1968 p. 558; Thwaites 1960, p. 418). Improvements to the aerodynamic characteristics of the spinning Frisbee have been attributed to spoilers that "disrupt the airflow" and "create a turbulent unseparated boundary layer over the convex side of the saucer and… result in a reduction of drag especially in high-speed flight and an increase in stability while in flight" (Headrick 1965). This description parallels the classical explanation of drag reduction wherein the drag coefficient of a body is reduced due to a tripping of the boundary layer to turbulent flow via high momentum mixing. This added momentum is said to cause the boundary layer to remain attached farther downstream on the body surface. It is clear that a lack of separation improves the drag characteristics of a body. The question remains as to what causes the lack of separation. The phrase "high momentum mixing," often used to explain this phenomenon, has not generally proved to be extremely useful from a predictive standpoint. More recent ring designs, based on the Frisbee concept, with a bulk

of material along the outer radius, appear to have even smaller drag coefficient. The enhanced flying characteristics of these designs are often attributed to the "spoiler" material on the outer rim. However, an equal, if not greater, effect of the massive outer rim is likely the prolonged rotation sustained by its flywheel affect. As noted by Potts and Crowther (2002), the distance record for a thrown Frisbee now stands at 250 m. The distance record for any hand-thrown object was set at 406.29 m in 2003 using the Aerobie Pro Ring and then at 427.2 m by Schummy (2005) using a boomerang. It seems unlikely that any non-rotating object could be thrown such distances, regardless of its shape or stability. Compare the above facts, for example, with the distance record for the javelin set at 98.48 m in 1996.

One of the more subtle but curious contributions provided by CFD studies in the last few decades has been the placing on fairly firm footing the concept observable in the experimental data presented by Swanson (1961) and Tanaka and Nagano (1972), namely that under certain conditions, rotation of a cylinder not only generates lift but also reduces drag (see, e.g., Ingham 1983, Diaz *et al.* 1985, Badr *et al.* 1989, Ingham and Tang 1990, D'Alessio and Dennis 1994, Kang and Choi 1999, Stojković *et al.* 2002, Stojković *et al.* 2003, Inoue *et al.* 2003, Mittal and Kumar 2003).

The major difficulty in theoretically predicting the flow properties for bluff-body flow problems lies in the separated boundary layer. Specific problems encountered when trying to apply conventional boundary layer theory to separated boundary layers include: a lack of knowledge of the proper far stream pressure boundary condition along the region leading up to separation, uncertainty as to the location of the point of separation, and uncertainty as to the pressure at which separation occurs.

Models of the wake aimed at predicting drag are numerous (Kirchhoff 1869, Joukowsky 1890, Riabouchinsky 1920, McNown and Yih 1953, Roshko 1954, Lavrentiev 1962, Wu 1962, Parkinson and Jandali 1970, Wu 1972, Yeung and Parkinson 1997). These rely heavily on a knowledge of the shape of the body in question. The closed wake model suggested by Batchelor (1956) focused primarily on finding the external flow past regions of uniform vorticity (see Childress 1966, Sadovskii 1971, Turfus 1993). Roshko (1993) derived an expression for the length of the mean wake bubble in terms of the base suction coefficient and Reynolds shear stress for a normal flat plate with a trailing splitter plate. Using the free streamline model, Roshko was then able to predict a reasonable value for the drag coefficient. However, it is difficult to extend the model to a wake without a splitter plate that experiences vortex shedding (Roshko 1993; Williamson 1996*a*). Balachandar *et al.* (1997) conducted a thorough review of past wake models and presented detailed contours of flow properties in the wake of cylinders and flat plates.

Correlations of drag versus flow speed for a given bluff-body shape are complicated by factors such as flow transitions, surface roughness effects, and the choosing of the proper characteristic length and area to be used in the Reynolds number and drag coefficient. Rotation effects present an added difficulty. For these reasons, no single correlation, empirical or otherwise, has been found to relate drag force to flow speed for different body shapes and for all flow speeds.

The goal of the present study is to arrive at a correlation between force and motion that is valid for various body shapes.

2. An Integral Quantity Characterizing Rotational Regions

The following parameter is defined in regions in which rotation is present:

$$G = \int_{\forall} \frac{e_K}{\omega} \, \mathrm{d}\forall \, . \tag{1}$$

In the definition of this parameter, which will be used later in the drag correlation, e_K is the kinetic energy per unit volume, ω is the vorticity magnitude, and $\forbidden$ is the volume of any material possessing rotation.

In Table 1, the quantity G is evaluated inside various rotating, non-translating shapes. For the rigid bodies listed in Table 1, as well as the elliptical patch of uniform vorticity in planar flow, the following relation is found to hold:

$$G \;=\; \frac{1}{4}L\,, \tag{2}$$

where L is the angular momentum of the body or material. Although G and L are both evaluated for the same volume of rotating material, the relation in (2) appears not to be a kinematic identity because, as seen from Table 1, it is not true for the core of Hill's spherical vortex (Hill 1894). The following relation, however, does hold for the spherical vortex as well as the solid cylinder and the elliptical patch of uniform vorticity:

$$L \;=\; \dot{m}S\,. \tag{3}$$

Here, S is the cross-sectional area of the vortex containing a mean circulating flow rate of $\dot{m}$. The mass flow rate $\dot{m}$ is that passing through the area $A = bW$, where W is the length of the vortex into the page (see Figure 1); therefore, $\forbidden = 2SW$ for a pair of identical vortices. Considering the complexity of the flow in the core of Hill's spherical vortex and the non-uniform distribution of mass flux along any axis from its core center to its perimeter, (3) is clearly not a trivial statement. The validity of (3) is naturally independent of the type of material enclosed.

Config.	$\dot{m}$	$\dfrac{\dot{m}}{m}$	$G = \displaystyle\int \frac{e_K}{\omega}\,\mathrm{d}\forbidden$	$L = \displaystyle\int \big\lvert\boldsymbol{\ell}\big\rvert\,\mathrm{d}\forbidden$	$\dfrac{G}{L}$
Elliptical vortex patch	$\dfrac{1}{2}\rho v_O b W$	$\dfrac{v_O}{2\pi\, a}$	$\dfrac{1}{8}\rho v_O \pi a b^2 W$	$\dfrac{1}{2}\rho v_O\, \pi a b^2 W$	$\dfrac{1}{4}$
Solid cylinder (radius = b)	$\dfrac{1}{2}\rho v_O b W$	$\dfrac{\Omega}{2\pi}$	$\dfrac{1}{8}\rho v_O \pi b^3 W$	$\dfrac{1}{2}\rho v_O\, \pi b^3 W$	$\dfrac{1}{4}$
Solid cone (base = b height = h)	$\dfrac{1}{6}\rho\Omega\, b^2 h$	$\dfrac{\Omega}{2\pi}$	$\dfrac{1}{40}\rho\Omega\pi b^4 h$	$\dfrac{1}{10}\rho\Omega\pi b^4 h$	$\dfrac{1}{4}$
Solid spinning sphere	$\dfrac{2}{3}\rho\Omega R^3$	$\dfrac{\Omega}{2\pi}$	$\dfrac{2}{15}\rho\Omega\,\pi R^5$	$\dfrac{8}{15}\rho\Omega\pi R^5$	$\dfrac{1}{4}$
Solid torus ($R_C \geq r_O$)	$\rho A\Omega R_C$	$\dfrac{\Omega}{2\pi}$	$\dfrac{\rho\Omega A\, C}{4}\left[\dfrac{3}{4}{r_O}^2 + {R_C}^2\right]$	$\rho\Omega A\, C\left[\dfrac{3}{4}{r_O}^2 + {R_C}^2\right]$	$\dfrac{1}{4}$
Spherical vortex (Hill 1894)	$\dfrac{\pi}{4}\rho v_O {R_O}^2$	$\dfrac{3\, v_O}{16 R_O}$	$\dfrac{\rho\pi^2 v_O {R_O}^4}{30}$	$\dfrac{\rho\pi^2 v_O {R_O}^4}{8}$	$\dfrac{4}{15}$

Table 1. Integral properties of rotating material in various shapes. (W is the length along the symmetry axis, $\Omega = v_O/b = v_O/R_O = v/R$, rotation is about the symmetry axis, $\boldsymbol{\ell} = R \times \rho v$, ρ and m are the density and mass of the material, respectively. For the torus: $A = \pi\, {r_O}^2$ is the torus cross-section area, and $C = 2\pi R_C$ is the circumference of the core circle. For Hill's spherical vortex, R_O is the sphere radius.)

3. Drag Correlation

In many bluff-body flow problems, general characteristics of the velocity field are fairly well known, at least in the region most critical to drag prediction, namely the wake bubble. In fact, the common trait among bluff-body flows appears to be the existence of a wake bubble in the time-mean flow field. For these reasons, a drag correlation is proposed in the present study that involves an integral property of the mean wake vortex, that is, either of the symmetric time-mean vortices in the wake bubble.

Figure 1 represent a stationary bluff body in which energy is contained within the wake bubble. As the wake bubble becomes fully turbulent with increasing Reynolds number, drag correlations involving the quantity $\dot{m}S$ in (3) become difficult to apply, while the quantity on the left side of (2) remains accessible. According to the far right column in Table 1, (2) cannot be assumed valid generally. However, in the present study, only two-dimensional bodies are considered; therefore, the spherical vortex is not immediately relevant.

Figure 2 shows the correlation of the quantity $c_D Re$ vs. $G/(\mu \forall)$ for various bluff bodies for which whole-field data is available in the literature. Here, c_D is the drag coefficient, μ is the fluid viscosity, and $\forall$ is the volume of either of the elliptical vortices in the time-mean wake bubble. The experimental data in Figure 2 suggest a relationship of the following form:

$$c_D\, Re \;=\; k \frac{G}{\mu \forall}. \tag{4}$$

In this context, the integration in (1) is carried out over the time-mean wake vortex. For this integration, the time-mean wake vortices trailing the symmetric bluff bodies were modeled by the elliptical patch of uniform vorticity, as explained in §4. Geometrical parameters of the pair of elliptical vortices, such as b/D (defined by Figure 1), were taken from the bluff-body wake measurements cited in the left-most column of Table 2.

Equation (4) may be cast in the form:

$$F_D = \frac{k\,G}{2S}\, v_\infty\,, \tag{5}$$

where F_D is the drag force, and v_∞ is the free stream velocity.

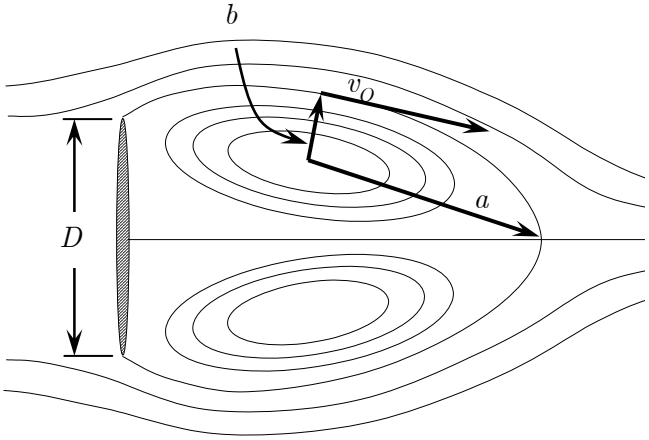

Figure 1. Schematic of flow past a normal flat plate.

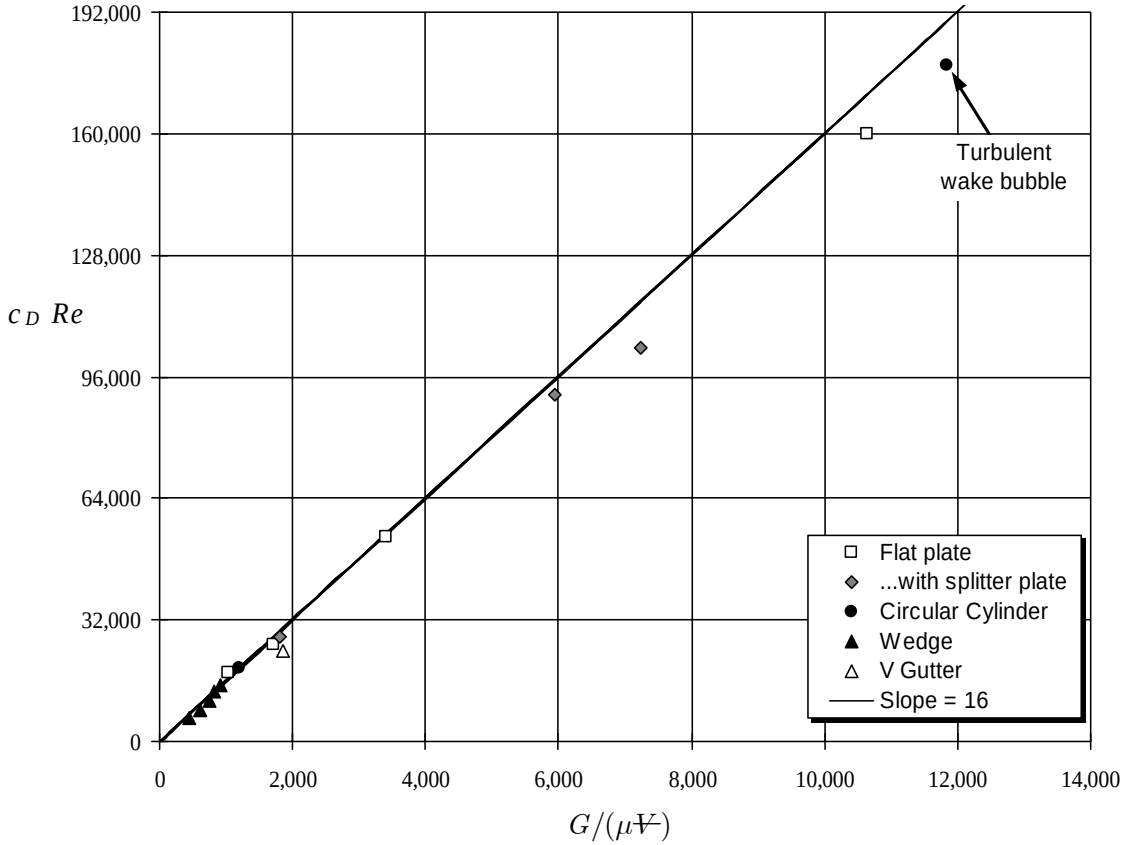

Figure 2. Variation of $c_D Re$ with $G/(\mu\forall)$ for various obstacles. Data references are tabulated in Table 2.

The far right column in Table 2, labeled "$c_{D\,data}$," shows values of drag coefficient obtained from the experimental studies listed in the left column of the table or in its footnotes. As seen from Figure 2, the data suggest that $k \approx 16$ in (4). The column labeled "$c_{D\,pred}$" in Table 2 shows values predicted by (4) with $k = 16$. (The actual equation used is (21), which is obtained by solving for c_D.)

The aspect ratio, AR, shown in Table 2 is defined as the ratio of the spanwise body dimension to its transverse dimension, and the blockage, β, is defined as the ratio of the transverse body dimension to the wind tunnel height measured in the same direction. All test bodies spanned the test sections or used end plates. Figure 3 shows the correlation of predicted and measured drag coefficient.

The correlation in (4) predicts a reduction in drag with increasing vorticity in the wake. It also suggests that a reduction in drag may be possible by increasing the vorticity in the wake of the body, such as by spinning the body appropriately. Such spinning of, for example, a disc upon re-entry into the atmosphere would also distribute the stagnation point along the entire perimeter of the body rather than confine it to a single point, thereby lowering the overall peak temperature. For the case of supersonic flight of such a spinning body, it is not yet known whether the sonic boom would be reduced relative to the non-spinning case.

Study	Geometry	Re	β	AR	St	a/D	b/D	v_O/v	$c_{D\,\mathrm{Pred}}$	$c_{D\,\mathrm{Data}}$
Arie & Rouse (1956)	Normal plate & splitter plate	75,000	8.3%	12			0.47	0.82	1.54	1.38[a]
Castro & Haque (1987)	Normal plate & splitter plate	23,000	6.5%	12.4			0.46	0.79	1.45	1.38[b]
Ruderich & Fernholz (1986)	Normal plate & splitter plate[c]	32,000	10%	22			0.55[d]	0.64[e]	1.44	n.a.
Good & Joubert (1968)	Normal fence in boundary layer	63,000	11%	11			0.72	1.05	1.51[f]	1.45[g]
Perry & Steiner (1987)	Flat plate	20,000	24.6%	9.4	0.17	1.1	0.29		1.36	1.27[h]
Leder & Geropp (1993)	Flat plate	28,000	8.5%	n.a.	0.14	1.32	0.42		1.95	1.92
Fail *et al.* (1957)	Flat plate	86,000	2.6%	29	0.145	1.6	0.33	0.75	1.92	1.86[i]
Bachalo *et al.* (1993)	Cylinder	16,000	16.4%	6.1	0.19	1.15	0.22		1.21	1.20
Cantwell & Coles (1983)	Cylinder	144,000	4%	29	0.179	0.43	0.12		1.31	1.237
Okamoto *et al.* (1977)	Wedge:									
	$\alpha = 15^o$	9,000	2.5%	40	0.245	0.525	0.25		0.81	0.68
	$\alpha = 30^o$	9,000	2.5%	40	0.24	0.69	0.26		1.08	0.91
	$\alpha = 60^o$	9,000	2.5%	40	0.214	0.88	0.285		1.35	1.19
	$\alpha = 90^o$	9,000	2.5%	40	0.179	1.01	0.32		1.45	1.45
	$\alpha = 120^o$	9,000	2.5%	40	0.164	1.1	0.355		1.61	1.64
	$\alpha = 180^o$	9,000	2.5%	40	0.143	1.25	0.41		1.84	2.01
Yang & Tsai (1992)	V-Gutter (30^o)	24,000	20%	5	0.225[j]	0.55	0.4		1.24	1.0[k]

Table 2. Comparison between the drag coefficient of various two-dimensional bodies and the values predicted by (21). $Re > 9{,}000$.

[a] This value obtained by Arie & Rouse omits the drag of their long ($10D$) splitter plate by virtue of the location at which they measured the downstream pressures in their drag integral.
[b] This value by Arie & Rouse (1956) omits the drag of the splitter plate ($17D$ in this case).
[c] Length of splitter plate = $30D$. Ruderich & Fernholz intentionally tested with very high free stream turbulence (30%).
[d] Figure 6 of Ruderich & Fernholz (1986).
[e] According to Figure 8 of Castro & Haque (1987), velocity profiles appear to cross at the common value of v_O at the vertical distance b from the vortex center to the wake bubble boundary. This fact was used to determine v_O from Figures 15 of Ruderich & Fernholz (1986). Note that the origins of velocity profiles in their figure are staggered across the top of the plot; the bottom gives the scale.
[f] The correlation value was divided in half because only one vortex was present.
[g] From Figure 6 of Good & Joubert (1968) with $h/\delta = 2.34$.
[h] Taken from Fail *et al.* (1957) data for appropriate aspect ratio.
[i] Their value of 1.96 based on Fage & Johansen (1927) was corrected for blockage by Fail *et al.* (1957) using Maskell's method (see Maskell 1965).
[j] Yang *et al.* (1994).
[k] Hoerner (1965) p. 3-18.

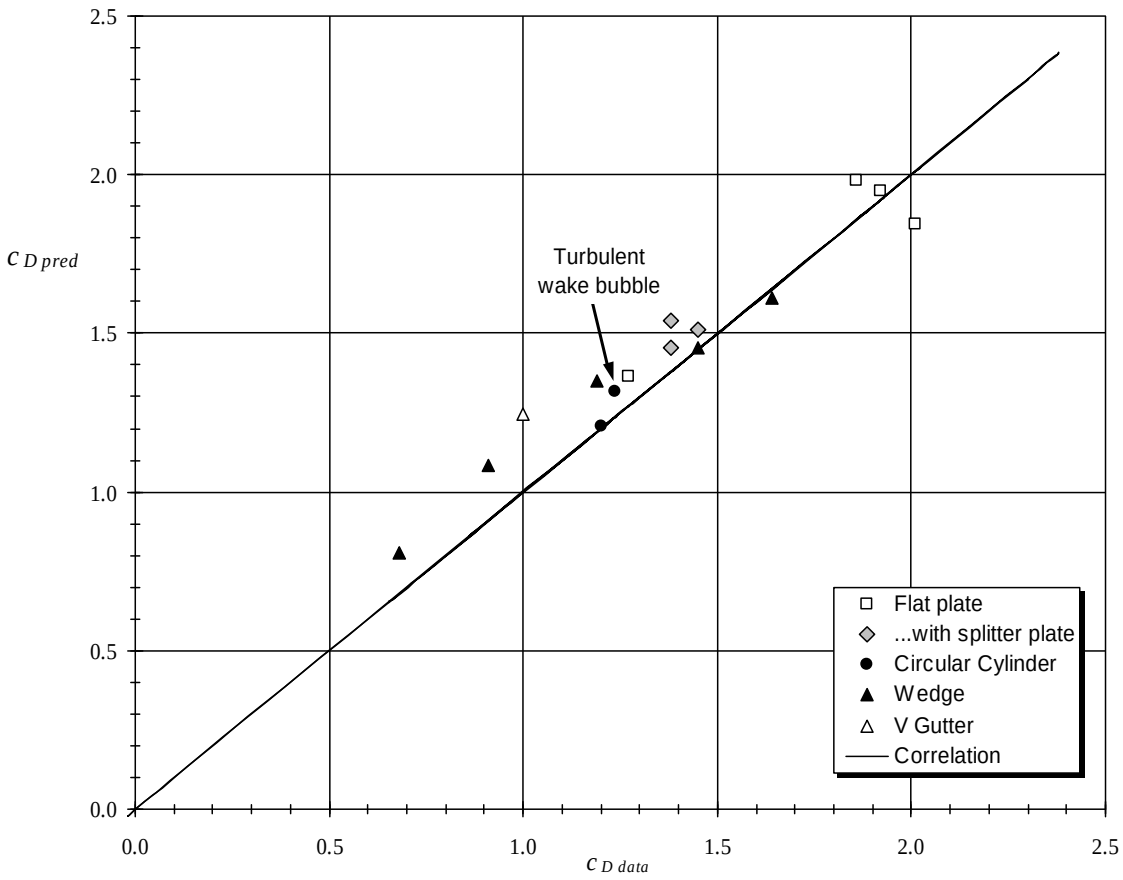

Figure 3. Correlation of predicted values of c_D with data listed in Table 2.

4. Evaluating G in a Planar Wake Vortex

Equation (4) or (5), together with the calculation of G to be described in §4.2, will relate the drag coefficient of two-dimensional bodies at high Reynolds numbers to an integral property of their wakes, expressed in terms of the velocity at a point on the perimeter of the time-mean wake vortex and a dimension of this vortex. The mean velocity field, required for the calculation of G, can be determined from the analytical solution for the flow field in the wake bubble. As observed by Roshko (1967), even for flows exhibiting vortex shedding, the time average in the near wake remains a pair of counter-rotating vortices (see also Perry and Steiner 1987). These are known experimentally to have a linear velocity profile along their semi-minor axes (see, e.g., Castro and Haque 1987, Yang and Tsai 1992). If this fact, along with the continuity equation, is applied to a stationary elliptical vortex, the resulting vorticity field is uniform (see Morton 1997). Therefore, for the nominally two-dimensional flows considered herein, the time-mean velocity field of the wake bubble can be approximated quite well using a pair of stationary elliptical patches of uniform vorticity. The velocity field in an elliptical patch of uniform vorticity can be found by constructing a streamlined coordinate system made of concentric elliptical streamlines and applying the continuity equation inside (see Morton 1997; also summarized in §4.1 below).

4.1. Velocity, Pressure, and Vorticity Fields in the Time-Mean Wake Vortex

A streamline coordinate system can be defined in a time-mean wake vortex as follows:

$$x = \overline{x}^1 A\cos(\overline{x}^2) \qquad y = \overline{x}^1 B\sin(\overline{x}^2) \qquad z = \overline{x}^3\,, \tag{6}$$

where x, y, and z are coordinates in a Cartesian system, and different values of the coordinate $\overline{x}^1$ correspond to different elliptical streamlines. Application of the continuity equation requires that the streamline component of the velocity tensor, $\mathrm{d}\overline{x}^k/\mathrm{d}t$, be (see Morton 1997):

$$\overline{v}^2 = \frac{v_O}{a}\,, \tag{7}$$

where $v_O = \Omega_O b$, the lengths a and b are, respectively, the semi-major and semi-minor axes of the elliptical vortex, and the superscript "2" on $\overline{v}^2$ is not an exponent but, rather, signifies the 2nd contravariant component of the velocity tensor. The quantity Ω_O is the rotation rate about the vortex center of a fluid particle at the point where the semi-minor axis intersects the perimeter of the vortex. Transforming from streamline coordinates to rectangular coordinates gives:

$$\boldsymbol{v} = \left[-y,\ \left(\frac{b}{a}\right)^2 x,\ \ 0\right]\Omega_O\,. \tag{8}$$

The pressure field in the vortex is (see Morton 1997):

$$p - p_C = \frac{1}{2}\rho\left(\Omega_O r\right)^2\left(\frac{b}{a}\right)^2\,, \tag{9}$$

where p is the pressure at a distance r from the vortex center where the pressure is p_C . Therefore, pressure contours are circular, regardless of the ellipticity of the vortex cross section. The constant vorticity of the elliptical patch is (see Morton 1997)

$$\omega \;=\; \overline{v}^2\left(\frac{a}{b} \;+\; \frac{b}{a}\right), \tag{10}$$

or

$$\omega \;=\; \frac{v_O}{b}\left[1 + \left(\frac{b}{a}\right)^2\right]. \tag{11}$$

4.2. Evaluating G

The ratio G to be used in (5) can be found by adding the turbulent kinetic energy per unit volume, e_{TK} , and the mean kinetic energy, e_{MK} , as follows:

$$G(1) \;\equiv\; \int\limits_{\forbar V(1)} \frac{e_K}{\omega}\,\mathrm{d}\forbar V \;=\; \int\limits_{\forbar V(1)} \left(\frac{e_{MK} \,+\, e_{TK}}{\omega}\right)\mathrm{d}\forbar V\,. \tag{12}$$

Here, the notation $G(1)$ signifies that only a single vortex is being considered at the moment. The standing eddies in symmetric bluff-body wakes naturally occur in pairs; therefore, for a pair of identical vortices,

$$G(2) \;=\; 2\int\limits_{\forbar V(1)} \left(\frac{e_{MK} \,+\, e_{TK}}{\omega}\right)\mathrm{d}\forbar V\,. \tag{13}$$

Here, ω is the absolute value of the vorticity. Expanding (13) gives

$$G(2) = \int_0^W \int_0^{2\pi} \int_0^{\bar{x}^1_{\max}} \frac{\overline{g}_{22}\left(\overline{v}^2\right)^2}{\sqrt{\overline{g}_{33}}\overline{\omega}^3} \rho\sqrt{\overline{g}}\,\mathrm{d}\overline{x}^1\mathrm{d}\overline{x}^2\mathrm{d}\overline{x}^3 \;+\; \int_{\text{eddy}} \frac{\left(\left\langle v_1'^{\,2}\right\rangle + \left\langle v_2'^{\,2}\right\rangle + \left\langle v_3'^{\,2}\right\rangle\right)}{\omega}\,\rho\,\mathrm{d}\forall\,, \quad (14)$$

where, for the streamlined coordinate system defined by (6), $\overline{g}_{33} = 1$, $\sqrt{\overline{g}} = \overline{x}^1 AB$, $\overline{\omega}^3 = \omega$ is the constant given by (10) or (11), and $\overline{g}_{22} = (\overline{x}^1)^2[A^2\sin^2(\overline{x}^2) + B^2\cos^2(\overline{x}^2)]$. The velocity components marked with primes in (14) indicate the random fluctuations of the respective components, and the angled brackets indicate averaging. According to (7), $\overline{v}^2$ is constant and, like $\overline{\omega}^3$, can be brought out of the integral. Performing the integration in (14) for the pair of vortices gives:

$$G(2) \;=\; \frac{1}{4}\rho v_O b\forall(1) \;+\; \frac{\rho {v_\infty}^2}{\omega} k_T\,\forall(1)\,, \quad (15)$$

where $\forall(1)$ is the volume of a single vortex, and

$$k_T \;\equiv\; \frac{1}{\forall(1)}\sum_i \left(\frac{\left\langle v_1'^{\,2}\right\rangle}{{v_\infty}^2} + \frac{\left\langle v_2'^{\,2}\right\rangle}{{v_\infty}^2} + \frac{\left\langle v_3'^{\,2}\right\rangle}{{v_\infty}^2}\right)\Delta\forall_i\,. \quad (16)$$

Notice from (15) that when turbulent kinetic energy is negligible in the wake vortex, the mean contribution to G, denoted hereafter as G_M, can be written as:

$$\frac{G_M(2)}{S} \;=\; \frac{\dot{m}(1)}{2}\,. \qquad \text{(planar, laminar pair)} \quad (17)$$

Since a pair of vortices will be considered from this point forward, the notation $G(2)$ will be replaced with simply G hereafter. Therefore, G_M/S is equal to half the mass flow rate through any semi-axis of either of the wake vortices. This fact was implied by (2) and (3). Generalizing (17) for N non-symmetrical wake vortices, one may write

$$\frac{G_M}{S} \;=\; \frac{1}{4}\sum_{i=1}^{N}\dot{m}_i\,, \qquad \text{(planar, laminar pair)} \quad (18)$$

where $\dot{m}_i$ is the mass flow rate in the ith wake vortex, and N is the number of vortices in the wake.

5. Drag Coefficient

The drag coefficient can be computed by substituting (11) into (15), and the result into (4), giving:

$$c_D \;=\; 8\frac{b}{D}\left[\frac{v_O}{2v_\infty} \;+\; \frac{2v_\infty}{v_O}\frac{k_T}{\left(1+(b/a)^2\right)}\right]. \quad (19)$$

In all of the cases studied herein, namely two-dimensional flows, the characteristic length D is the projected body dimension normal to the free stream and is used in the Reynolds number. In all values of Table 2, except for those of Cantwell and Coles (1983) (which will be discussed in §6 and §7), the turbulent transition waves (Bloor 1964) had not penetrated into the wake vortex so that $k_T = 0$ in those cases.

If the velocity ratio appearing in (19) is not known, it can often be related to the shedding frequency by a Strouhal number grouping derived from the elliptical vortex patch (see Appendix). The necessary relation from that derivation is repeated below for convenience:

$$\frac{v_O}{v_\infty} = \frac{2\pi a}{nD}\,St\,. \tag{20}$$

Here, St is the classical definition of the Strouhal number, and n is the number of vortices shed downstream per shedding cycle, namely 2. Equation (20) can be employed to write (19) in terms of the Strouhal number rather than the vortex perimeter velocity ratio. With the onset of vortex shedding, however, the energy becomes split into a mean component and a periodic component. The mean wake bubble dramatically decreases in size with the removal of a splitter plate. This is clearly demonstrated by Hwang *et al.* (2003) at lower Reynolds number. If the correlation for the drag coefficient, (19), is modified so as to fit the data in Table 2 with and without splitter plates, the following form is obtained:

$$c_D \;=\; 8\,\frac{b}{D}\left[(1+\delta)\,\frac{v_O}{2v_\infty} \;+\; \frac{2\,v_\infty}{v_O}\,\frac{k_T}{\left(1+(b/a)^2\right)}\right]. \tag{21}$$

When vortex shedding is absent due to the presence of a splitter plate and the attendant large wake bubble, $\delta = 0$; and when vortex shedding is present and the mean wake bubble shrinks, $\delta = 1$. Therefore, for a non-turbulent wake bubble, kinetic energy of the mean flow is cut in half when the splitter plate is removed, the missing half being in the form of vortex shedding. Since all non-turbulent kinetic energy is accounted for (in the present work) by considering only the time-mean wake bubble, the kinetic energy due to vortex shedding must be included separately through the use of δ.

In summary, using (21), drag predictions can be made from steady or time-mean wake flow visualizations; however, the perimeter velocity, v_O , must be measured experimentally. The dimensionless distance, b/D, to this point from the vortex center may be found graphically from visualization of the mean flow (see Figure 1). Alternatively, by using (20), the measured Strouhal number and dimensionless semi-major axis, a/D, of the wake vortex may be used in lieu of the velocity ratio.

6. Illustrative Example

The case to be examined is the set of cylinder experiments made by Cantwell and Coles (1983). The purpose of their experiment was to provide measurements of wake flow in which the separation point was laminar, yet the near wake region was fully turbulent. Perrin *et al.* (2006) made a similar comprehensive study of the cylinder in cross flow at essentially the same Reynolds number but with low aspect ratio and higher blockage. In accordance with their objective stated above, Cantwell and Coles chose from a series of cases, one in which the Reynolds number was 1.44×10^5 so that the flow was on the brink of entering the so-called drag crisis.

Table 3 shows values reported by Bearman (1969) for the Strouhal number and drag coefficient on either side of this drag crisis. The mean velocity measurements of Cantwell and Coles (1983) immediately below the flow speed at which this drag crisis occurs are shown in Figure 4 with a indicated. Since the velocity at the semi-minor axis of the wake vortex was not given, (20) will be used to estimate it.

Re	c_D	St
2×10^5	1.14	0.19
4.1×10^5	0.235	0.46

Table 3. Values of drag coefficient and Strouhal number before and after the drag crisis. (Bearman 1969)

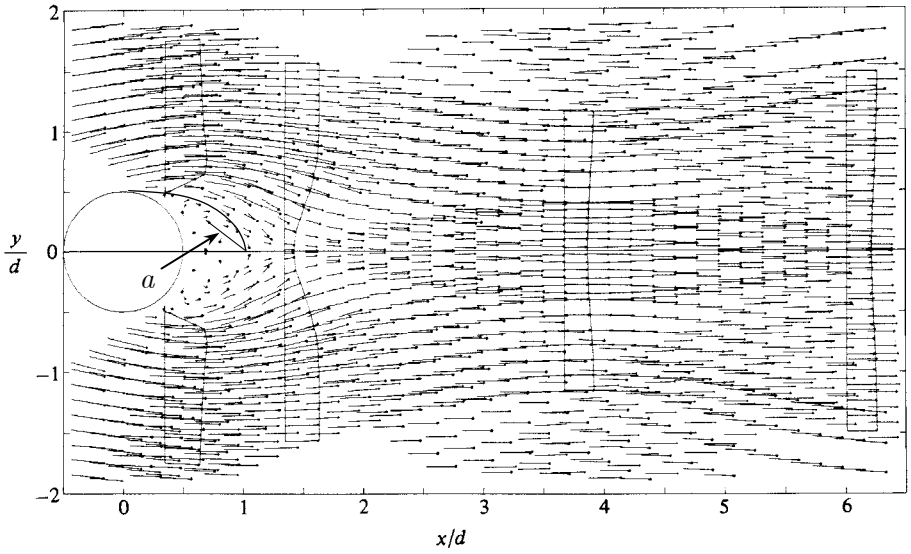

Figure 4. Mean velocity vectors in the wake of a circular cylinder. $Re = 144{,}000$, $AR = 25$, $\beta = 4\%$, $c_D = 1.237$, $St = 0.179$, $TL = 0.6\%$. (adapted from Cantwell and Coles 1983)

At this Reynolds number, the turbulent transition waves have penetrated the wake bubble. The result is a noticeable reduction in the size of the wake bubble and a dramatic increase in the *fluctuating* component of velocity. Measurements of the needed velocity fluctuations were also made by Cantwell and Coles. The turbulent kinetic energy in the wake bubble can be found using mean contours of the random fluctuations $\langle v_1'^{\,2} \rangle / {v_\infty}^2$ and $\langle v_2'^{\,2} \rangle / {v_\infty}^2$, shown (with overbars) in Figures 27(b) and 28(b) of their paper. The remaining quantity, $\langle v_3'^{\,2} \rangle / {v_\infty}^2$, will be assumed to be an average of these two. The Reynolds normal stress contours reported by Cantwell and Coles (1983) appear very similar to those presented by Perrin *et al.* (2006) for a low aspect ratio cylinder and by Balachandar *et al.* (1997) for a cylinder wake bubble at low Reynolds number. From these and Figure 4 above, the semi-axes of the vortices are found graphically to be $a \,/\, D \approx 0.43$ and $b \,/\, D \approx 0.12$. Applying (16) graphically to Figures 27(b) and 28(b) of Cantwell and Coles (1983) shows that $k_T = 0.147$.

The velocity ratio v_O / v_∞ is found using (20):

$$\frac{v_O}{v_\infty} = \frac{2\pi\big(0.43\big)}{2} 0.179 = 0.242 \,.$$

The drag coefficient can then be estimated by (21), as follows:

$$c_D \;=\; 8\,\frac{b}{D}\left[(1+\delta)\frac{v_O}{2v_\infty} \;+\; \frac{2v_\infty}{v_O}\,\frac{k_T}{\Big(1+(b\,/\,a)^2\Big)}\right]$$

$$c_D \;=\; 8\,(0.12)\left[(1+1)\frac{0.242}{2} \;+\; \frac{2}{0.242}\,\frac{(0.147)}{\Big(1+(0.279)^2\Big)}\right]$$

$$c_D \;\approx\; 1.31$$

The value measured by Cantwell and Coles was $c_D = 1.237$.

7. Discussion

7.1. The Drag Crisis

In the example shown, the drag coefficient remains large even after the increase in the turbulent kinetic energy within the wake bubble and the decrease in mean wake width. The drag coefficient finally decreases suddenly when the Reynolds number is increased still further into the range $2 \times 10^5 < Re < 5 \times 10^5$, known as the "drag crisis," due to the well-known shift in the location of the separation point. This shift causes the circulation (effectively the denominator of (5)) to increase suddenly. Recall that the Reynolds number in the Cantwell and Coles experiment was large enough for the mean wake bubble to become almost entirely turbulent, yet small enough to ensure that the separation point remain forward on the body. The range of Reynolds numbers for which this set of circumstances exists is narrow. At these unique conditions, the size of the wake bubble is much smaller than it is at slightly lower Reynolds numbers, for which the wake bubble is not fully turbulent. Therefore, as the Reynolds number is increased into this unique range, the increase in fluctuating kinetic energy in the wake bubble and the reduction in the size of the mean wake bubble occur simultaneously, with no noticeable change in the drag coefficient. The circulation in the wake bubble, on the other hand, has not changed appreciably within this narrow range of Reynolds numbers because circulation within the wake volume is a direct function of the distance traveled by the fluid through the boundary layer. The sudden reduction in the drag coefficient does not occur until the boundary layer extends to the rear of the cylinder, at an even higher Reynolds number. The distance traveled by the fluid in the boundary layer is then longer, the circulation in the denominator of the drag relation is therefore higher, and hence the drag coefficient suddenly decreases (see (4)). Therefore, the decrease in drag coefficient occurs at a slightly higher Reynolds number than does the decrease in wake size. Consequently, near the drag crisis, the reciprocal of circulation appears to be a much stronger predictor of drag than the mean wake size.

Situations do exist where advancement of the transition point forward on the body has the effect of reducing drag (see e.g., Coustols 1996, Gad-el-Hak & Bushnell 1991, Coustols and Schmitt 1990). However, this is accomplished by placing distributed roughness elements or riblets on the surface, which can themselves be viewed from the standpoint of increasing the circulation in the fluid and hence reducing the drag.

7.2. Turbulent Angular Momentum

For turbulent flows, the drag correlation is easier to evaluate using the left side of (2) than the right. However, if the right side of (2) is substituted into (5), one obtains:

$$F_D = 2\, v_\infty \frac{L}{S}, \tag{22}$$

for each half of the wake bubble. Therefore, for a given velocity, a higher force causes a higher angular momentum per unit area of wake cross section. Turbulence is an ideal mechanism for filling a region with concentrations of angular momentum to accommodate a large force. From Table 1 and (3), we can write

$$\dot{m} = \frac{L}{S} = \frac{1}{2}\rho v_O b W \tag{23}$$

for a cylindrical vortex, the cross section of which is depicted in Figure 5*a*. If this cylindrical vortex shown were replaced with two counter-rotating vortices, as shown in Figure 5*b*, while maintaining the same velocity magnitude at points of tangency, the length b would become half of what it was in Figure 5*a*, as shown. There would be no gain in the storage capacity of angular momentum per unit area, L/S, (or mass flow rate) because, while there are now twice as many vortices, the quantity L/S, which according to (23) scales with b, is cut in half

for each vortex. If, however, the original vortex were replaced with four vortices, as shown in Figure 5*c*, there would be a gain in storage capacity of mass flow rate because b in this case reduces to $b/(1+\sqrt{2})$, and consequently the mass flow rate $\dot{m}(1)$ circulating in a single vortex decreases by the same ratio, $1/(1+\sqrt{2})$. Yet there are now $N=4$ vortices. Therefore, the total storage capacity of mass flow rate increases by a factor of $4/(1+\sqrt{2})$, since $\dot{m} = \sum \dot{m}(1) = N\dot{m}(1)$.

In the limit as the number of vortex cross sections filling a given area increases, that is, as $N \to \infty$, we find by equating the total vortex cross-sectional areas before and after this subdivision process that the radius, and hence the mass flow rate $\dot{m}(1)$ of each small vortex, scales as $\dot{m}(1) \sim 1 \,/\, \sqrt{N}$, so that the total storage capacity of mass flow rate within the volume scales as $\dot{m} \sim N\dot{m}(1) \sim \sqrt{N}$. Therefore, according to these very rough order-of-magnitude arguments, *the total mass flow rate enclosed in the wake volume can increase without bound as the vortices become smaller.*

If the initial region were to subdivide into spherical rather than tubular vortices, the mass flow rate within each small vortex would scale as $\dot{m}(1) \sim R^2$ according to Table 1. Equating the volumes before and after the subdivision process shows that the radius of each smaller spherical vortex scales as $R \sim 1 \,/\, N^{1/3}$. Therefore, the mass flow rate within each of these vortices scales as $\dot{m}(1) \sim R^2 \sim 1 \,/\, N^{2/3}$, so that the total storage capacity of mass flow rate in the volume scales as $\dot{m} \sim N\dot{m}(1) \sim N^{1/3}$. Therefore, again, the mass flow rate increases without bound as the number of vortices in a given region increases.

In general, therefore,

$$R \;\sim\; \frac{1}{N^{1/n}}\,, \tag{24}$$

$$\dot{m} = \sum_{i=1}^{N} \dot{m}(1) = N\dot{m}(1) \;\sim\; N^{1/n}\,, \tag{25}$$

where n is the dimensionality of the vortex, and R is the radius of the vortex, whether tubular ($n=2$) or spherical ($n=3$). Therefore, even though N is greater for a packing of spherical vortices than for a packing of cylindrical vortex tubes of equal radius, as shown in the preceding paragraphs, the mass flow rate in each of the N vortex *tubes* is likely greater than it is in each of the N *spherical* vortices, the general relation being: $\dot{m}(1) \sim 1/N^{(n-1)/n}$. Substituting (24) into (25) shows that the two effects exactly compensate one another so that the total mass flow rate in the wake increases as $1/R$, where R is the radius of the small vortices, whether tubular or spherical.

In §3, it was stated that drag correlations using $\dot{m}$ are difficult to apply to highly turbulent wake bubbles, yet the correlation using G, which employs the ratio of kinetic

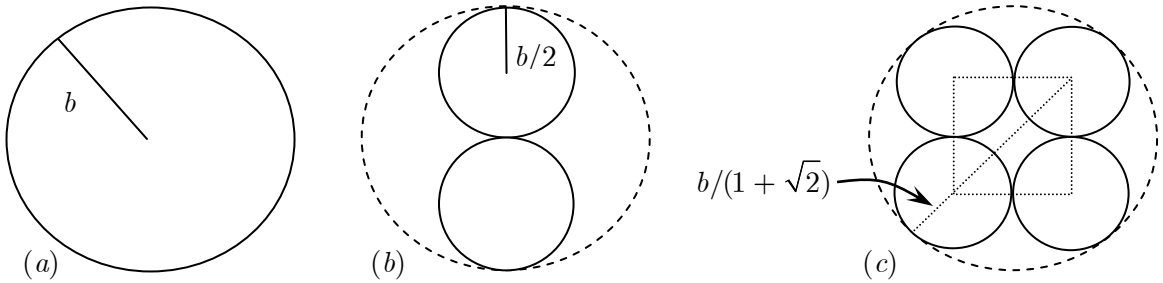

Figure 5. Model of the subdivision process of a single vortex into multiple smaller vortices. (*a*) $N=1$, (*b*) $N=2$, (*c*) $N=4$.

energy to circulation, remains measurable (recall that there is no distinction in these two for a laminar vortex). This is because calculating $\dot{m}$ for a turbulent wake bubble based upon Figure 5*a* is inaccurate (and counting turbulent eddies in the equivalent of Figure 5*c* is impractical).

Substitution of (3) into (22) gives, for both halves of the wake bubble:

$$F_D = 4\,\dot{m}\,v_\infty\,, \tag{26}$$

where $\dot{m}$ is now defined as the *total* mass flow rate circulating *in all* eddies in the wake bubble. If a relation such as (26) or (5) should turn out to be valid generally, not only would it relate drag to flow speed without the use of viscosity, but, in the form of (26), it may be useful in turbulence modeling or as an eddy size criterion in large eddy simulation studies.

In turbulent flows, the quantity $\dot{m}$ cannot be computed reliably by assuming a flux across a semi-axis of wake vortices. If the wake bubble is so chaotic that $\dot{m}$ cannot be estimated, the ratio of kinetic energy to circulation contained in (1) provides a reasonably measurable alternative quantity which seems to serve the same purpose as $\dot{m}$.

7.3. Extending the Correlation to Lower Reynolds Numbers

At Reynolds numbers lower than those studied here, there are complex transitions that make it difficult to evaluate G in the wake. For a description of the changes occurring in the wake during these transitions, see Williamson (1996*a* or 1996*b*) for the circular cylinder and Julien *et al.* (2003) for the flat plate. In order to better understand the three-dimensional behavior of flow in the near wake of a normal flat plate, Wu *et al.* (2005) analyzed the phase difference of vortex shedding at two different spanwise locations and found two distinct modes and very pronounced three-dimensionality. These two distinct shedding modes, also reported by Najjar and Balachandar (1998), may be related to the effect originally reported by Fail *et al.* (1957). In particular, Fail *et al.* noted that there are generally two shedding frequencies for each plate, "one associated with the smaller dimension of the plate, and a lower frequency associated with the larger dimension."

At low flow speeds where changes occur in the nature of out-of-plane shedding, the correlation underpredicts the drag coefficient by as much as a factor of 2. Beyond $Re \sim \mathrm{O}(10^3)$ on the other hand, any contribution due to out-of-plane energy appears to remain a constant fraction of the total as flow speed changes, so that the correlation need only consider that in the nominal flow plane.

8. Conclusion

The drag of two-dimensional bodies appears to be correlated with the ratio of the kinetic energy to the vorticity in its wake, at least in the range $9\times10^3 \le Re \le 1.44\times10^5$. (Note, however, that with only a single data point corresponding to a turbulent wake, more empirical evidence is needed to confidently extend the correlation into the turbulent wake regime.) To make calculation of the ratio possible from whole-field data from the literature, all vorticity is assumed to reside in the mean wake bubble. At lower Reynolds numbers (not studied here), this assumption becomes more difficult to justify. As a limiting case of the drag correlation, ideal flows possess infinitely thin boundaries and therefore infinite vorticity in these boundaries, and hence no drag. To evaluate the correlation parameter, G, the mean wake bubble was modeled as a pair of elliptical patches of uniform vorticity. To aid in computing the required correlation parameter from existing test data, a Strouhal number defined in terms of the elliptical vortex patch can be used in lieu of the time-averaged velocity at a point on the vortex perimeter. This Strouhal number remains constant under all conditions. The correlation indicates that the drag force on a body is proportional to the flow speed and the mass flow rate in the wake bubble. Absent any quantization of vortex size, this

mass flow rate, and hence the drag force, can become unbounded as the scale of the contained vortices becomes finer.

Appendix: A Universal Strouhal Number

In cases where the quantities necessary for calculating G in the mean recirculation region are reported directly from experimental studies, the following discussion is unnecessary. However, since these values are rarely available, the quantities must be deduced from available measurements in the wake.

In order to relate the time-mean wake vortex to the instantaneous vortex shedding, it is important to realize that the period, $T_{\rm v}$, of the pair of elliptical vortices, which constitute the time-mean recirculation region, is related to the period, T_s, of the vortex shedding. In nominally planar flow, the period, $T_{\rm v}$, of the time-mean elliptical vortex can be determined by integrating (7) around any elliptical streamline (since all of them have the same period), as follows:

$$\int_0^{2\pi} \mathrm{d}\overline{x}_2 = \int_0^{T_{\rm v}} \frac{v_O}{a}\,\mathrm{d}t \tag{27}$$

$$\therefore\ T_{\rm v} = \frac{2\pi a}{v_O}. \tag{28}$$

Recall that a is the maximum radius of the time-mean elliptical wake vortex, and v_O is the maximum velocity on its perimeter (at the minimum radius). With n vortices shed downstream per shedding cycle, we also have:

$$T_{\rm v} = \frac{n}{f_s} \tag{29}$$

where f_s is the vortex shedding frequency. Here, we have effectively equated the period of the time-mean vortex to the period of one shedding cycle in the instantaneous flow. Eliminating $T_{\rm v}$ from (28) and (29) suggests the following potentially useful grouping:

$$S \equiv \frac{f_s\, a}{v_O} = \frac{n}{2\pi} \approx 0.318\,. \tag{30}$$

The weak Reynolds number dependence of the classical Strouhal number for a circular cylinder in the range $(3\times10^2 < Re < 10^5)$ has led several researchers (Roshko 1954; Bearman 1967; Griffin 1981; Adachi *et al.* 1996) to define variants of Strouhal's dimensionless grouping in order to obtain a quantity that can be reliably considered constant under all conditions. These are referred to as "universal Strouhal numbers" (see also the review by Buresti 1983). The quantity S defined by (30) represents yet another such dimensionless grouping. The unique feature of (30), however, is that it truly takes a constant value in all nominally two-dimensional bluff body flows, namely $1/\pi$. The dimensionless grouping in (30) is equal to the characteristic frequency of the time-mean vortex (and the shedding frequency in the instantaneous flow) divided by the vortex eigenvalue, $\lambda = \pm i\, v_O/a$, of the system $\dot{\boldsymbol{x}} = \boldsymbol{A}\,\boldsymbol{x}$ represented by (8). The near constancy of other Strouhal number groupings is due to the fact that they use length and velocity scales that are closely related to those of the eigenvalue of the time-mean wake vortex. The same period is implied in (30) whether shedding is present or not. For Reynolds numbers at which vortex shedding occurs, this period is the reciprocal of the shedding frequency; below this Reynolds number range, it is the period of the standing eddies.

The foregoing can be used to relate shedding frequency observations to the velocity ratio required by the correlation in (19), unless a splitter plate trails the body, in which case the primary vortex shedding is eliminated. Solving (30) for v_O gives:

$$v_O = \frac{2\pi}{n} a f_s = \frac{2\pi a}{nD} St\, v_\infty$$

$$\therefore \frac{v_O}{v_\infty} = \frac{2\pi a}{nD} St\,, \tag{31}$$

where St is the classical definition of the Strouhal number. Combining this relation with the solution (8) for a stationary elliptical vortex allows the velocity field in the wake vortex to be estimated by measurements of the Strouhal number.

References

Adachi, T., Ozaki, T., Yamamoto, T., Eguchi, Y., Matsuuchi, K., & Kawai, T., "Study of the Universal Strouhal Number over the Wide Reynolds Number Flow Range, (Effect of Surface Roughness)," *JSME International Journal B* **39**, (2) (1996) pp. 335-342. [15]

Arie, M., & Rouse, H., "Experiments on two-dimensional flow over a normal wall," *Journal of Fluid Mechanics* **1** (1956) pp. 129-141. [6]

Bachalo, W. D., Bachalo, E. J., Hanscom, J. M., & Sankar, S. V., "An Investigation of Spray Interaction With Large-Scale Eddies," *AIAA Paper No. 93-0696* (1993) 19 pp. [6]

Badr, H. M., Dennis, S. C. R., & Young, P. J. S., "Steady and unsteady flow past a rotating circular cylinder at low Reynolds numbers," *Computers & Fluids* **17** (1989) pp. 579-609. [2]

Balachandar, S., Mittal, R., & Najjar, F. M., "Properties of the mean recirculation region in the wakes of two-dimensional bluff bodies," *Journal of Fluid Mechanics* **351** (1997) pp. 167-199. [2, 11]

Batchelor, G. K., "A proposal concerning laminar wakes behind bluff bodies at large Reynolds numbers," *Journal of Fluid Mechanics* **1** (1956) pp. 388-398. [2]

Bearman, P. W., "On vortex street wakes," *Journal of Fluid Mechanics* **28** (1967) pp. 625-641. [15]

Bearman, P. W., "On vortex shedding from a circular cylinder in the critical Reynolds number régime," *Journal of Fluid Mechanics* **37** (1969) pp. 577-585. [10]

Bloor, M. S., "The transition to turbulence in the wake of a circular cylinder," *Journal of Fluid Mechanics* **19** (1964) pp. 290-304. [9]

Bradbury, L. J. S., "Measurements with a pulsed-wire and a hot-wire anemometer in the highly turbulent wake of a normal flat plate," *Journal of Fluid Mechanics* **77** (1976) pp. 473-497. [6]

Buresti, G., "Appraisal of Universal Wake Numbers From Data for Roughened Circular Cylinders," *Journal of Fluids Engineering* **105** (1983) pp. 464-468. [15]

Cantwell, B. J., & Coles, D., "An experimental study of entrainment and transport in the turbulent near wake of a circular cylinder," *Journal of Fluid Mechanics* **136** (1983) pp. 321-374. [6, 9-12]

Castro, I. P. & Haque, A., "The structure of a turbulent shear layer bounding a separation region," *Journal of Fluid Mechanics* **179** (1987) pp. 439-468. [6, 7]

Childress, S., "Solutions of Euler's Equations containing Finite Eddies," *Physics of Fluids* **9** (1966) pp. 860-872. [2]

Coustols, E., "Riblets: main known and unknown features," in *Emerging techniques in drag reduction*, Mechanical Engineering Publications, London, edited by Choi, Prasad, and Truong (1996) pp. 3-43. [1, 12]

Coustols, E. & Schmitt, V., "Synthesis of Experimental Riblet Studies in Transonic Conditions," in *Turbulence Control by Passive Means, Proceedings of the 4th European Drag Reduction Meeting*, Kluwer Academic Publishers, Dordrecht, edited by E. Coustols (1990). [12]

D'Alessio, S. J. D. & Dennis, S. C. R., "A vorticity model for viscous flow past a cylinder," *Computers & Fluids* **23** (1994) pp. 279-293. [2]

Davies, J. M., "The Aerodynamics of Golf Balls," *Journal of Applied Physics* **20** (1949) p. 821-828. [1]

Diaz, F., Gavaldà, J., Kawall, J. G., Keffer, J. F., & Giralt, F., "Asymmetrical Wake Generated by a Spinning Cylinder," *AIAA Journal* **23** (1985) pp. 49-54. [2]

Djenidi, L., Anselmet, F., Liandrat, J., & Fulachier, L., "Laminar boundary layer over riblets," *Physics of Fluids* **6** (1994) pp. 2993-2999. [1]

Fage, A. & Johansen, F. C., "On the Flow of Air behind an Inclined Flat Plate of Infinite Span," *Proceedings of the Royal Society of London A* **116** (1927) pp. 170-197. [6]

Fail, R., Lawford, J. A., & Eyre, R. C. W., "Low-Speed Experiments on the Wake Characteristics of Flat Plates normal to an Air Stream," *Aeronautical Research Council, Reports and Memoranda* No. 3120 (1957). [6, 14]

Gad-el-Hak, M. & Bushnell, D. M., "Separation Control: Review," *ASME Journal of Fluids Engineering* **113** (1991) pp. 5-30. [12]

Good, M. C. & Joubert, P. N., "The form drag of two-dimensional bluff-plates immersed in turbulent boundary layers," *Journal of Fluid Mechanics* **31** (1968) pp. 547-582. [6]

Griffin, O. M., "Universal Similarity in the wakes of Stationary and Vibrating Bluff Structures," *Journal of Fluids Engineering* **103** (1981) pp. 52-58. [15]

Headrick, E. E., "Flying Saucer," *U.S. Patent No. 3,359,678* (1967). [1]

Hill, M. J. M., "On a Spherical Vortex," *Philosophical Transactions of the Royal Society of London A* **185** (1894) pp. 213-245. [3]

Hoerner, S. F., *Fluid-Dynamic Drag*, published by Hoerner Fluid Dynamics (1965). [6]

Hwang, J.-Y, Yang, K.-S., & Sun, S.-H., "Reduction of flow-induced forces on a circular cylinder using a detached splitter plate," *Physics of Fluids* **15** (2003) pp. 2433-2436. [10]

Ingham, D. B., "Steady flow past a rotating cylinder," *Computers & Fluids* **11** (1983) pp. 351-366. [2]

Ingham, D. B. & Tang, T., "A Numerical Investigation into the Steady Flow Past a Rotating Circular Cylinder at Low and Intermediate Reynolds Numbers," *Journal of Computational Physics* **87** (1990) pp. 91-107. [2]

Inoue, O., Mori, M., & Hatakeyama, N., "Control of aeolian tones radiated from a circular cylinder in a uniform flow," *Physics of Fluids* **15** (2003) pp. 1424-1441. [2]

Joukowsky, N. E., "I - A modification of Kirchhoff's method of determining a two-dimensional motion of a fluid given a constant velocity along an unknown streamline, II - Determination of the motion of a fluid for any condition given on a streamline," *Matematicheskii Sbornik* **15** (1890) pp. 121-278; (also *Collected Works of N. E. Joukowsky*, Vol. II, III, Issue 3, *Trans. CAHI* (*Central Aero-Hydrodynamical Institute*), Moscow, No. 41, 1930.) [2]

Julien, S., Lasheras, J., & Chomaz, J.-M., "Three-dimensional instability and vorticity patterns in the wake of a flat plate," *Journal of Fluid Mechanics* **479** (2003) pp. 155-189. [14]

Kang, S. & Choi, H., "Laminar flow past a rotating circular cylinder," *Physics of Fluids* **11**, pp. 3312-3321; 2000, "Erratum," *Physics of Fluids* **11** (1999) pp. 239-240. [2]

Kirchhoff, G., "Zur Theorie freier Flüssigkeitsstrahlen," *Journal fuer die reine und angewandte Mathematik* (*Crelle*) **70** (1869) pp. 289-298. [2]

Lavrent'ev, M. A., "The variational method in boundary-value problems for systems of equations of elliptic type," *Izdat. Akad. Nauk SSSR*, Moscow (1962) 136 pp., (in Russian). [2]

Leder, A. & Geropp, D., "Analysis of Unsteady Flows Past Bluff Bodies," *Journal of Wind Engineering and Industrial Aerodynamics* **49** (1993) pp. 329-338. [6]

Maskell, E. C., "A Theory of the Blockage Effects on Bluff Bodies and Stalled Wings in a Closed Wind Tunnel," *Aeronautical Research Council, Reports and Memoranda* No. 3400 (1965), (supersedes some older ARC reports, 25 pp.). [6]

McNown, J. S. & Yih, C-S., "Free-streamline analyses of transition flow and jet deflection," *Engineering Bulletin* **35**, State Univ. of Iowa (1953). [2]

Milne-Thomson, L. M., *Theoretical Hydrodynamics*, 5th edition, Dover, NY (1968). [1]

Morton, T. S., "Application of an Elliptical Vortex Solution to a New Universal Strouhal Number and a Scalar Invariant for Drag Prediction," Ph.D. Dissertation, Brigham Young University (1997). [1, 7-8]

Najjar, F. M. & Balachandar, S., "Low-frequency unsteadiness in the wake of a normal flat plate," *Journal of Fluid Mechanics* **370** (1998) pp. 101-147. [14]

Okamoto, T., Yagita, M., & Ohtsuka, K., "Experimental Investigations of the Wake of a Wedge," *Bulletin of the JSME* **20**, (141) (1977) pp. 323-328. [6]

Parkinson, G. V. & Jandali, T., "A wake source model for bluff body potential flow," *Journal of Fluid Mechanics* **40** (1970) pp. 577-594. [2]

Perrin, R., Braza, M., Cid, E., Cazin, S., Moradei, F., Barthet, A., Sevrain, A., & Hoarau, Y., "Near-Wake Turbulence Properties in the High Reynolds Number Incompressible Flow Around a Circular Cylinder Measured by Two- and Three-Component PIV," *Flow, Turbulence and Combustion* **77** (2006) pp. 185-204. [10, 11]

Perry, A. E. & Steiner, T. R., "Large-scale vortex structures in turbulent wakes behind bluff bodies. Part 1. Vortex formation processes," *Journal of Fluid Mechanics* **174** (1987) pp. 233-270. [6, 7]

Potts, J. R. & Crowther, W. J., "Frisbee™ Aerodynamics," *AIAA-2002-3150* (2002) 15 pp. [2]

Riabouchinsky, D., "On steady fluid motions with free surfaces," *Proceedings of the London Mathematical Society* **19** (1920) pp. 206-215. [2]

Roshko, A., "A new hodograph for free streamline theory," *NACA Technical Note* 3168 (1954). [2, 15]

Roshko, A., "A review of concepts in separated flow," *Proc. Can. Cong. Appl. Mech., Quebec* **3** (1967) pp. 81-115. [7]

Roshko, A., "Perspectives on bluff body aerodynamics," *Journal of Wind Engineering and Industrial Aerodynamics* **49** (1993) pp. 79-100. [2]

Ruderich, R. & Fernholz, H. H., "An experimental investigation of a turbulent shear flow with separation, reverse flow, and reattachment," *Journal of Fluid Mechanics* **163** (1986) pp. 283-322. [7]

Sadovskii, V. S., "Vortex regions in a potential stream with a jump of Bernoulli's constant at the boundary," *Applied Mathematics and Mechanics* **35** (1971) pp. 729-735. [2]

Schummy, D., *Guinness World Records* 2006, Guinness (2005). [2]

Stojković, D., Breuer, M., & Durst, F., "Effect of high rotation rates on the laminar flow around a circular cylinder," *Physics of Fluids* **14** (2002) pp. 3160-3178. [2]

Stojković, D., Schön, P., Breuer, M., & Durst, F., "On the new vortex shedding mode past a rotating circular cylinder," *Physics of Fluids* **15** (2003) pp. 1257-1260. [2]

Swanson, W. M., "The Magnus Effect: A Summary of Investigations to Date," *ASME Journal of Basic Engineering, D* **83** (1961) pp. 461-470. [2]

Tanaka, H. & Nagano, S., "回転円柱まわりの流れに関する研究" ("Research on flow around rotating circular cylinders"), *Nippon Kikai Gakkai Ronbunshu* **38** (1972) pp. 1343-1352 (in Japanese). [2]

Thwaites, B., *Incompressible Aerodynamics*, Clarendon, Oxford (1960). [1]

Turfus, C., "Prandtl-Batchelor flow past a flat plate at normal incidence in a channel – inviscid analysis," *Journal of Fluid Mechanics* **249** (1993) pp. 59-72. [2]

Walsh, M. J. & Lindemann, A.M., "Optimization and application of riblets for turbulent drag reduction," *AIAA Paper No. 84-0347* (1984). [1]

Williamson, C. H. K., "Vortex dynamics in the cylinder wake," *Annual Review of Fluid Mechanics* **28** (1996*a*) pp. 477-539. [2, 14]

Williamson, C. H. K., "Three-dimensional wake transition," *Journal of Fluid Mechanics* **328** (1996*b*) pp. 345-407. [14]

Wu, S. J., Miau, J. J., Hu, C. C., & Chou, J. H., "On low-frequency modulations and three-dimensionality in vortex shedding behind a normal plate," *Journal of Fluid Mechanics* **526** (2005) pp. 117-146. [14]

Wu, T. Y., "A wake model for free-streamline flow theory Part 1. Fully and partially developed wake flows and cavity flows past an oblique flat plate," *Journal of Fluid Mechanics* **13** (1962) pp. 161-181. [2]

Wu, T. Y., "Cavity and wake flows," *Annual Review of Fluid Mechanics* **4** (1972) pp. 243-284. [2]

Yang, J.-T., & Tsai, G.-L., "The Wake Flow Structure of an Open-Slit V Gutter," *Experimental Thermal and Fluid Science* **5** (1992) pp. 685-696. [6, 7]

Yang, J.-T., Tsai, G.-L., & Wang, W.-B., "Near-Wake Characteristics of Various V-Shaped Bluff Bodies," *Journal of Propulsion and Power* **10** (1994) pp. 47-53. [6]

Yeung, W. W., H. & Parkinson, G. V., "On the steady separated flow around an inclined flat plate," *Journal of Fluid Mechanics* **333** (1997) pp. 403-413. [2]